Structural Model of Porcine Factor VIII and Factor VIIIa Molecules Based on Scanning Transmission Electron Microscope (STEM) Images and STEM Mass Analysis

Michael W. Mosesson, David N. Fass,* Pete Lollar,‡ James P. DiOrio, Carlo G. Parker,‡ Gaylord J. Knutson,* James F. Hainfeld,§ and Joseph S. Wall§

*University of Wisconsin Medical School-Milwaukee Clinical Campus, Milwaukee, Wisconsin 53233; *Mayo Clinic/Foundation, Rochester, Minnesota 55905; ‡University of Vermont, Burlington, Vermont 05405; and §Brookhaven National Laboratory, Upton, New York 11973*

Abstract

Porcine plasma factor VIII (fVIII) molecules are heterodimers composed of a 76,000-mol wt light chain ($-A_3-C_1-C_2$) and a heavy chain ranging in molecular weight from 82,000 (A_1-A_2) to 166,000 (A_1-A_2-B). Proteolytic activation of fVIII by thrombin results in fVIIIa heterotrimers lacking B domains (A_1, A_2, $A_3-C_1-C_2$). In this study, immunoaffinity purified fVIII was further fractionated by mono S or mono Q chromatography to prepare heterodimers containing a light chain and an A_1-A_2-B heavy chain (fVIII 166/76) or an A_1-A_2 heavy chain (fVIII 82/76). Mass analysis of scanning transmission electron microscopic (STEM) images of fVIII 166/76 indicated that heterodimers (mass 237±20 kD) had irregularly globular core structures 10–12 nm across, and frequently displayed a diffuse, occasionally globular to ovoid satellite structure extending 5–14 nm from the core, and attached to it by a thin stalk. Factor VIII 82/76 molecules (mass 176±20 kD) had the same core structures as fVIII 166/76 molecules, but lacked the satellite structure. These findings indicate that A_1-A_2 domains of heavy chains and the light chains of the fVIII procofactor molecule are closely associated and constitute the globular core structure, whereas the B domainal portion of heavy chains comprises the peripheral satellite appendage. Factor VIII core structures commonly displayed a finger-like projection near the origin of the B domainal stalk that was also a consistent feature of the free heavy chains (mass 128–162 kD) found in fVIII 166/76 preparations. Factor VIII light chain monomers (mass, 76±16 kD) were globular to c-shaped particles 6–8 nm across. These chains commonly possessed a v-shaped projection originating from its middle region, that could also be observed at the periphery of fVIII core molecules. Factor VIIIa preparations contained heterotrimers (mass 162±13 kD) that had the same dimensions as fVIII core structures, lacked the B domainal appendage, and sometimes possessed the same core features as fVIII molecules. Molecular species corresponding to heterodimers (mass, 128±13 kD) and unassociated subunit chains (40–100 kD) were also observed in fVIIIa preparations, suggesting that heterotrimers have an appreciable tendency to dissociate, a phenomenon that could explain the decay of fVIIIa activity after thrombin activation of fVIII. (*J. Clin. Invest.* 1990. 85:1983–1990.) electron microscopy • scanning transmission electron microscopy • factor VIII • factor VIIIa

Introduction

Factor VIII (fVIII)[1] is a plasma glycoprotein that is absent or abnormal in hemophilia A. In humans, it is synthesized as a mature polypeptide chain of 2,332 amino acids and contains three types of domains (i.e., A, B, C) in the sequence $NH_2-A_1-A_2-B-A_3-C_1-C_2-COOH$ (1, 2) (Fig. 1). Because of cleavages between the B and A_3 domains, perhaps occurring intracellularly (4), fVIII exists in porcine plasma as a divalent cation-linked heterodimer comprised of a heavy chain of variable size and a light chain ($-A_3-C_1-C_2$) of mol wt 76,000 (5). Heavy chain size heterogeneity is due to proteolytic cleavages within the B domain resulting, with respect to porcine fVIII, in heavy chain peptides of mol wt 166,000 (A_1-A_2-B), 130,000 (A_1-A_2-B/), or 82,000 (A_1-A_2) (5, 6). Likewise, human fVIII molecules are heterodimeric, having subunits similar in size to those of porcine fVIII (1, 7–10).

The molecular weight of partially to highly purified human or porcine fVIII, based upon hydrodynamic parameters (7, 10–12) or upon radiation inactivation experiments (13, 14), has been estimated to lie between 140,000 and 285,000. The rather wide range of values obtained may depend to some extent (e.g., reference 7) upon the size heterogeneity of heavy chain components. Summation of the molecular weights of the various constituents of porcine fVIII molecules yields values ranging from 158,000 (A_1-A_2,$-A_3-C_1-C_2$) to 242,000 (A_1-A_2-B,$-A_3-C_1-C_2$) (5, 6).

The addition of thrombin to fVIII causes a rapid increase in procoagulant fVIIIa activity, and is accompanied by cleavage between the A_2 and B domains, between the A_1 and A_2 domains, and near the NH_2 terminus of the A_3 domain (Fig. 1) (1, 3). The resulting fVIIIa molecules form heterotrimers consisting of two heavy chain fragments (A_1, A_2) plus a light chain component ($A_3-C_1-C_2$), having a molecular weight of 161,000, as determined by sedimentation equilibrium analysis (15). Although thrombin activation is associated with proteolysis of its constituent peptides (5, 8, 12) and reduction of its size (11, 12, 15, 16), loss of fVIIIa activity after activation (6,

This work was presented in part at the 12th Congress of the International Society on Thrombosis and Haemostasis, 19–25 August, 1989 (1989. *Thromb. Haemostasis* 62:200), and at the 31st Annual Meeting of the American Society of Hematology, 2–5 December 1989 (1989. *Blood.* 74[Suppl. 1]:131a).

Address reprint requests to Dr. Mosesson, Sinai Samaritan Medical Center, 905 North Twelfth Street, Milwaukee, WI 53233.

Received for publication 27 October 1989 and in revised form 30 December 1989.

J. Clin. Invest.

0021-9738/90/06/1983/08 $2.00
Volume 85, June 1990, 1983–1990

1. *Abbreviations used in this paper:* fVIII, factor VIII; fVIIIa, factor VIIIa; STEM, scanning transmission electron microscopy.

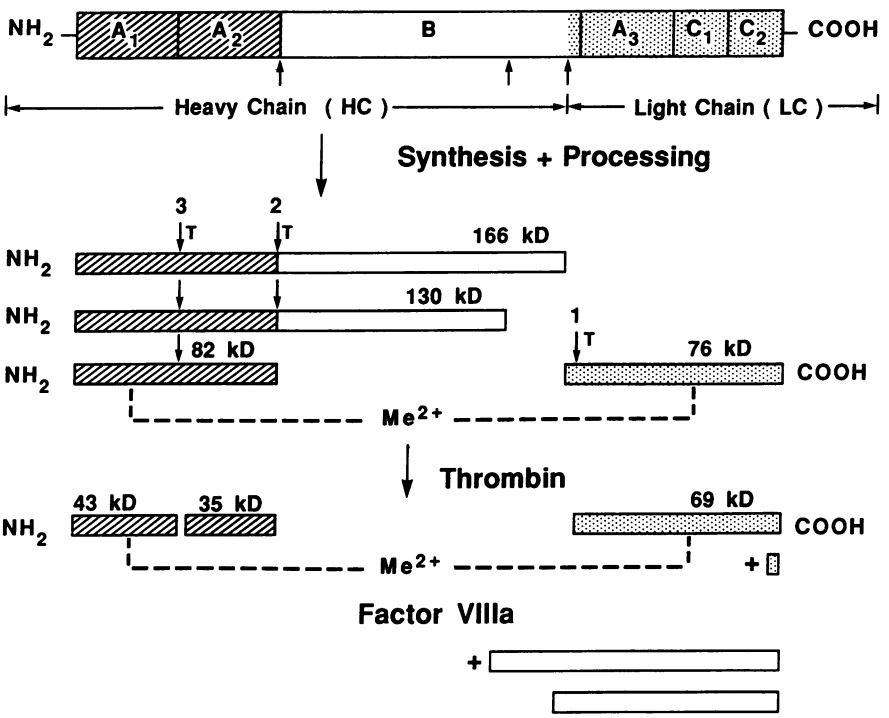

Figure 1. Schematic model of the domainal structure of single-chain fVIII and the structures of the three commonly identified heterodimeric fVIII molecules that are isolated from porcine plasma. Cleavages of single chain fVIII that result in the heavy and light chain populations found in plasma are indicated, as well as thrombin (*T*) cleavages of the heavy and light chains that accompany its activation to fVIIIa (1, 3). Heavy chains and light chains are linked noncovalently by a divalent cation (Me^{2+})-dependant mechanism. Large heavy chains containing B domainal structures are designated A_1–A_2–B (mol wt 166,000) or A_1–A_2–B/ (mol wt 130,000); small heavy chains, A_1–A_2 (mol wt 82,000); fVIII light chains, –A_3–C_1–C_2 (mol wt 76,000); fVIIIa light chains, A_3–C_1–C_2 (mol wt 69,000).

17–21) is not prevented by inhibitors of thrombin (11, 21). This indicates that loss of activity is not due to continued proteolysis by thrombin, a conclusion also supported by the results of Lollar et al. (6), who showed that factor IXa and phospholipid in the presence of calcium ions stabilized the activity of thrombin-activated porcine fVIIIa, although the size of fVIIIa components, as determined by SDS gel electrophoresis, did not differ from that of fVIIIa activated in the presence of thrombin alone.

Immunoaffinity chromatography of partially purified porcine fVIII has provided an effective method for purifying stable, though heterogeneous, fVIII (5). Further processing of immunoaffinity-purified fVIII by HPLC on mono S or mono Q columns has permitted separation of biologically active material into discrete subpopulations of heterodimers, and removal of a high molecular weight constituent devoid of coagulant activity (7, 15, 22). In addition, highly stable and active fVIIIa preparations have been prepared by HPLC of thrombin-activated fVIII on mono S columns (15). One of the main objectives of studying highly purified and stable components of fVIII and fVIIIa has been to facilitate elucidation of their structure in relation to their coagulant function. In this investigation, we have approached that objective using scanning transmission electron microscopy (STEM) coupled with STEM mass analysis to identify and characterize the ultrastructure of fVIII, fVIIIa, and their constituent peptides. A structural model of fVIII based upon these observations is offered.

Methods

Preparation of porcine fVIII and fVIIIa. Immunoaffinity-purified porcine fVIII was prepared as described (5) using a monoclonal antibody to the fVIII light chain (W3-3) that had been bound to Sepharose 4B (Pharmacia, Inc., Piscataway, NJ). This material was further chromatographed on a mono S or mono Q column (Pharmacia, Inc.; reference 15) to remove a high molecular weight constituent lacking fVIII activity, and to isolate a fVIII heterodimer fraction with a predominant heavy chain population of 166 kD (fVIII 166/76), and one with an 82 kD heavy chain (fVIII 82/76) (Fig. 2). Three such preparations were stored at 5°C in 10 mM histidine, 5 mM $CaCl_2$, pH 6.0 buffer, containing 0.5–0.7 M NaCl (mono S) or in 20 mM Tris, 5 mM $CaCl_2$, 0.7 M NaCl, pH 7.4 buffer (mono Q) at concentrations of 46–280 μg/ml. Factor VIIIa was prepared by chromatography on a mono S column as described (15) and stored at 5°C at concentrations of 80 or 173 μg/ml (two preparations). Factor VIII light chains (one preparation) were prepared as described (15) and stored at 5°C in 20 mM Tris, 5 mM $CaCl_2$, 0.45 M NaCl, pH 7.4 buffer at a concentration of 140 μg/ml.

STEM. High-resolution STEM was performed at the Brookhaven National Institutes of Health Biotechnology Resource Facility. The preparation of ultrathin carbon films and the method of specimen preparation and application for freeze-drying were as described (23, 24). Briefly, protein solutions for analysis were diluted to a final concentration of 5–10 μg/ml with 0.15 M NaCl, 1 mM $CaCl_2$, 10 mM Hepes buffer, pH 7.0, and injected into a droplet of the same buffer on a grid coated with an ultrathin (~ 3 nm) carbon film. After a 1-min attachment time, the specimen on the film was washed 8–10 times with 50 mM ammonium acetate, pH 7.0 solution to remove nonvolatile salts, freeze-dried slowly overnight, transferred to the STEM micro-

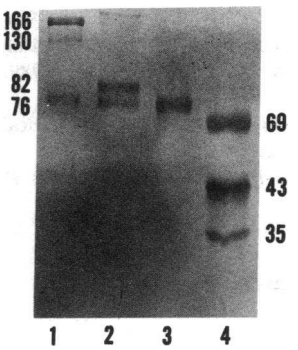

Figure 2. Composite SDS Laemmli PAGE of the nonreduced silver-stained fVIII, fVIIIa, and fVIII light chain preparations used in this study. The apparent molecular weights ($\times 10^{-3}$) of the components are indicated. Lane *1*, fVIII 166/76; lane *2*, fVIII 82/76; lane *3*, fVIII light chains; lane *4*, fVIIIa.

scope stage (−140°C) under vacuum, and imaged using a 40-kV probe focused at 0.25 nm. For some experiments, specimen wash solutions also contained 1 mM $CaCl_2$.

Image resolution under the specimen sampling conditions (1 nm/pixel) and the electron beam dose we used (1,000 e^-/nm^2) was ~ 2 nm (24). Particle mass measurements were performed off-line using a "circle of integration" program (23–25) with a variable integration radius depending upon the shape and area covered by any given object. Tobacco mosaic virus particles that had been added to the specimen were used as an internal mass calibration standard (26, 27). The accuracy of STEM mass measurements ranges from ± ~ 15 kD at an integration radius (r_i) of 10 nm to ± ~ 25 kD at an r_i of 20 nm (24). The mean mass values reported for the various populations of molecules found within a specimen were computed over a range of values that encompassed the species of interest.

STEM images were reproduced from a televised tape file onto Polaroid type 665 film and the negative was then acquired through a video camera (DAGE-MTI, Michigan City, IN) into an image processing system (model 8502, Tracor Northern, Middleton, WI). The images were then filtered to reduce background noise using a nonlinear grey level contrast processing program, and occasionally were smoothed using a median smoothing function to reduce the prominence of pixel lines. The filtered images were recovered by photographing the processed images on the computer TV screen. Assessments of the presence and form of subdomainal molecular features were made from filtered images.

Results

Factor VIII. Mass analysis of images of a fVIII 166/76 preparation revealed particles in a range of 70–450 kD (Fig. 3). The

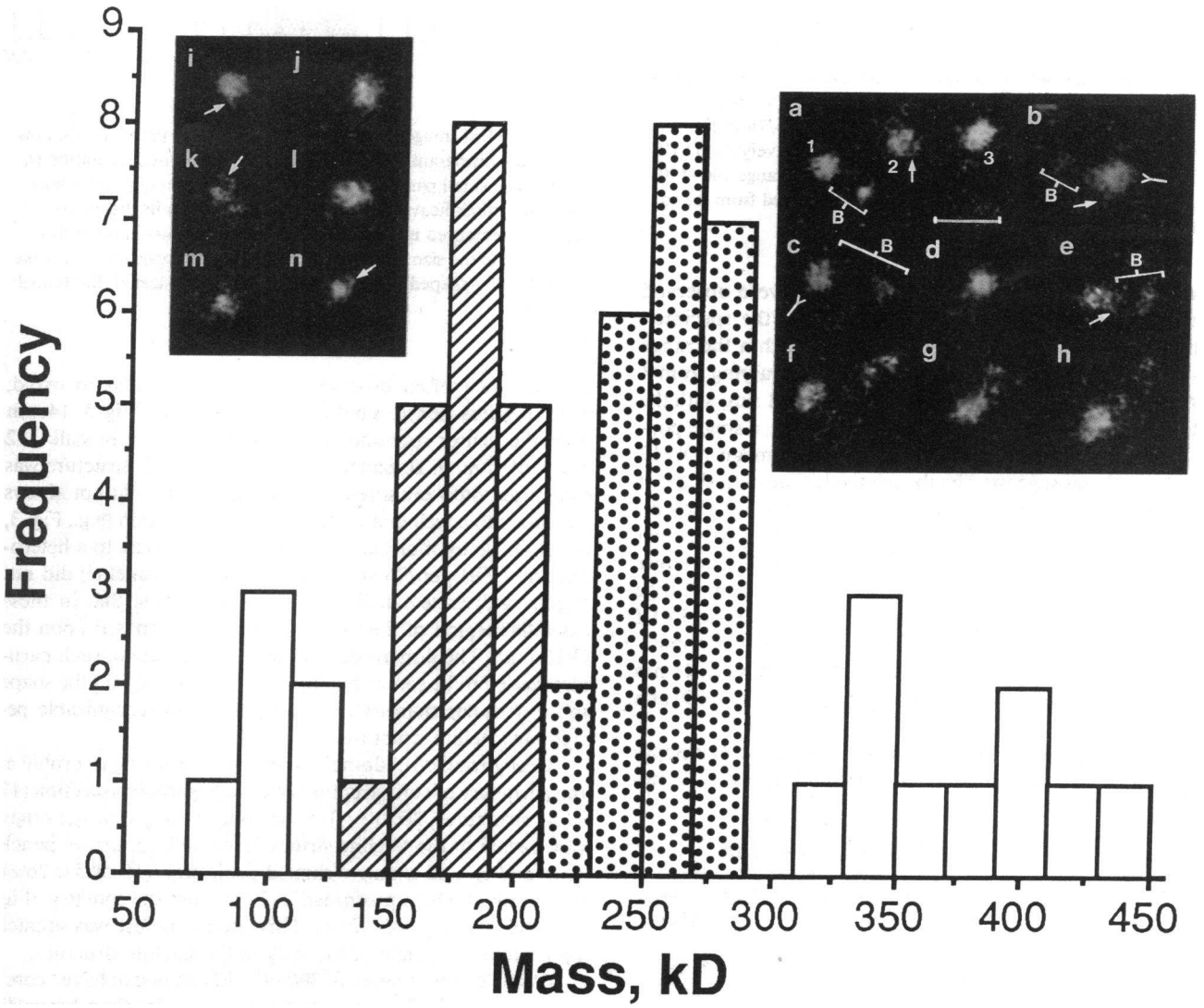

Figure 3. STEM images selected from fVIII 166/76 preparations, plus a frequency histogram of the size distribution (number of particles vs. mass) of particles in one such preparation (r_i 18 nm). The data in this histogram were obtained from a different fVIII 166/76 preparation than that presented in Fig. 4 and in the text. The pattern of particle distribution is essentially the same for both, but the mean value for the mass in the range 210–290 kD is insignificantly higher, 255±22 kD, than that found for the preparation reported in Fig. 4, 237±20 kD. The value in the 130–210-kD range, 179±20 kD, is virtually the same as in the preparation reported in Fig. 4, 177±19 kD. Panels *a–e* represent molecules selected from the size range shown by the dot filled bars, except in panel *a* in which only molecule *1* (58 kD) fulfills that requirement. Molecule *2* (162 kD) represents a free heavy chain, whereas molecule *3* represents a small fVIII heterodimer (193 kD). Panels *f–h* show molecules in the size range > 350 kD. Panels *i–n* were selected from the size range shown by the *striped bars,* and correspond to free heavy chains (*k–n*) and small factor VIII heterodimers (*i* and *j*). *Arrows* indicate fingerlike structures; *split lines,* v-shaped structures. Satellite structures are indicated by the brackets labeled *B.* Bar (panel *a*), 20 nm.

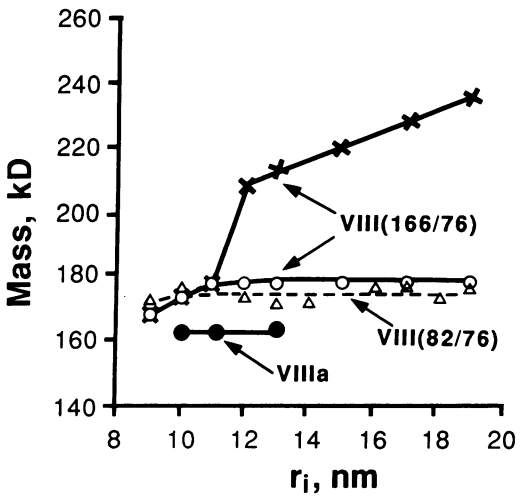

Figure 4. Mass of particles observed in fVIII and fVIIIa preparations plotted as a function of the radius of integration (r_i). Two populations of molecules found in a preparation of fVIII 166/76 in the range 120–290 kD are designated by × and ○, respectively; (△) fVIII 82/76 (range 140–220 kD); (●) fVIIIa heterotrimers (range 140–190 kD). The standard error for these measurements ranged from ±2 to ±8 kD.

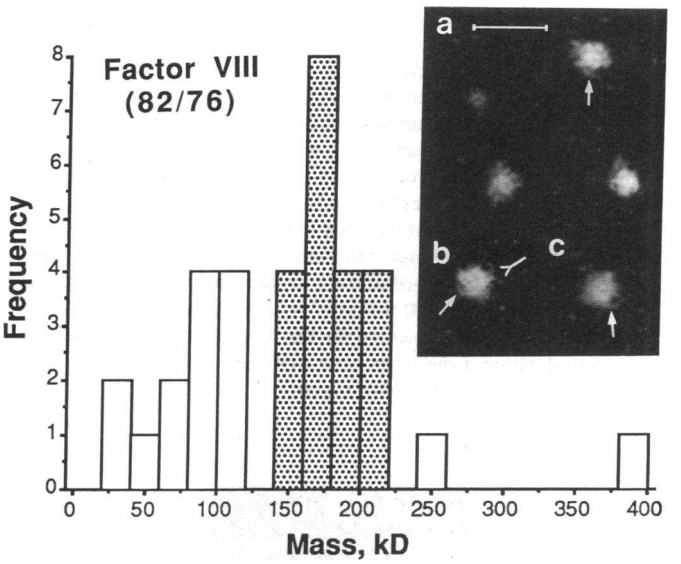

Figure 5. STEM images selected from fVIII 82/76 preparations, plus a frequency histogram of the mass of particles in one preparation (r_i 11 nm). The small particle in the upper left portion of panel *a* may represent a small heavy chain (A_1–A_2), based upon its distinctive shape and measured mass, 68 kD. The *dot-filled bars* in the histogram indicate the size range of the other particles selected. Fingerlike (*arrows*) and v-shaped (*split line*) structures are indicated. Bar (panel *a*), 20 nm.

same mass distribution and particle shapes were observed whether or not 1 mM $CaCl_2$ was included in the specimen wash buffer (data not shown). Most objects within the range 130–290 kD were irregularly globular particles varying from 8 to 14 nm across. At an integration radius of 9–11 nm, with the circle of integration centered about these objects, a single population of molecules between 140 and 220 kD (mean 178±17 kD; r_i 11 nm) was suggested by the relatively Gaussian shape of this portion of the frequency histogram (data not shown). However, as the integration radius was increased, two distinct size populations of molecules were revealed (Fig. 4). The larger population had a mass of 237±20 kD at r_i 19 nm (range 210–290 kD), and corresponded to heterodimeric fVIII 166/76 molecules (Table I). The mass of the second population of molecules did not increase significantly above r_i, 11 nm and had a mean value of 177±19 kD (range 120–200 kD) at r_i 19 nm.

Examination of the larger fVIII 166/76 heterodimer population revealed irregular globular core structures 8–12 nm across, which often possessed a smaller, globular to ovoid, relatively less dense, satellite structure extending 5–14 nm from the denser core and connected to it by a thin stalk 1–2 nm wide (Fig. 3, *B*, panels *a, b, c,* and *e*). This structure was sometimes diffusely spread on the surface and did not always terminate in a well-defined globular configuration (e.g., Fig. 3, panel *f*). Many molecules corresponding in mass to a heterodimeric fVIII 166/76 structure (e.g., Fig. 3, panel *d*) did not display a discrete satellite structure, suggesting that in these cases this region of the molecule was superimposed upon the fVIII core. The dimensions of the core structure of such particles tended to be somewhat larger (up to 14 nm) and the shape more irregular than that of molecules with recognizable peripheral satellite structures.

Recognizable subdomainal features appearing in profile at the periphery of core structures were a fingerlike projection (17 of 56 structures; 30%) ~ 3–5 nm long, arising near the origin of the stalk of the satellite structure (e.g., Fig. 3, *arrow,* panels *b, e,* and *i*), and a thin v-shaped projection (15 of 57; 26%), each limb of which protruded 2–3 nm from the core (e.g., Fig. 3, panels *b* and *c, split lines*). This latter structure was situated opposite to the origin of the stalk of the satellite structure.

Particles with masses of 300–450 kD tended to have "core" structures that were larger and more irregular than heterodimeric fVIII 166/76 structures (Fig. 3, panels *g* and *h*), consistent with them representing aggregates of two fVIII 166/76 molecules or perhaps two or more heavy chains, or some combination of these. Some heterodimeric fVIII 166/76 molecules with a high mass were situated so near to other smaller structures that both were included in the mass measurement (e.g., Fig. 3, panel *f*). Particles with masses < 110 kD represented 5–7% of the objects observed, and were not investigated further in these studies.

Table I. Mass of Porcine Factor VIII and Factor VIIIa

Preparation	Values for molecular weight × 10^{-3} (ref.)	Mass determined by STEM
fVIII 166/76	242* (5, 6)§	237±20
fVIII 82/76	158* (5, 6)§	176±20
fVIIIa	154* (5, 6); 161‡ (15)	162±13‖

* Values determined by summation of constituent subunits, whose sizes were determined by SDS gel electrophoresis.
‡ Value determined from hydrodynamic measurements.
§ Aronson et al. (13) estimated the molecular weight of unsubfractionated porcine or human fVIII to be 180,000 from radiation inactivation experiments.
‖ Value determined for heterotrimers; the mass of heterodimers was 128 ± 13 kD.

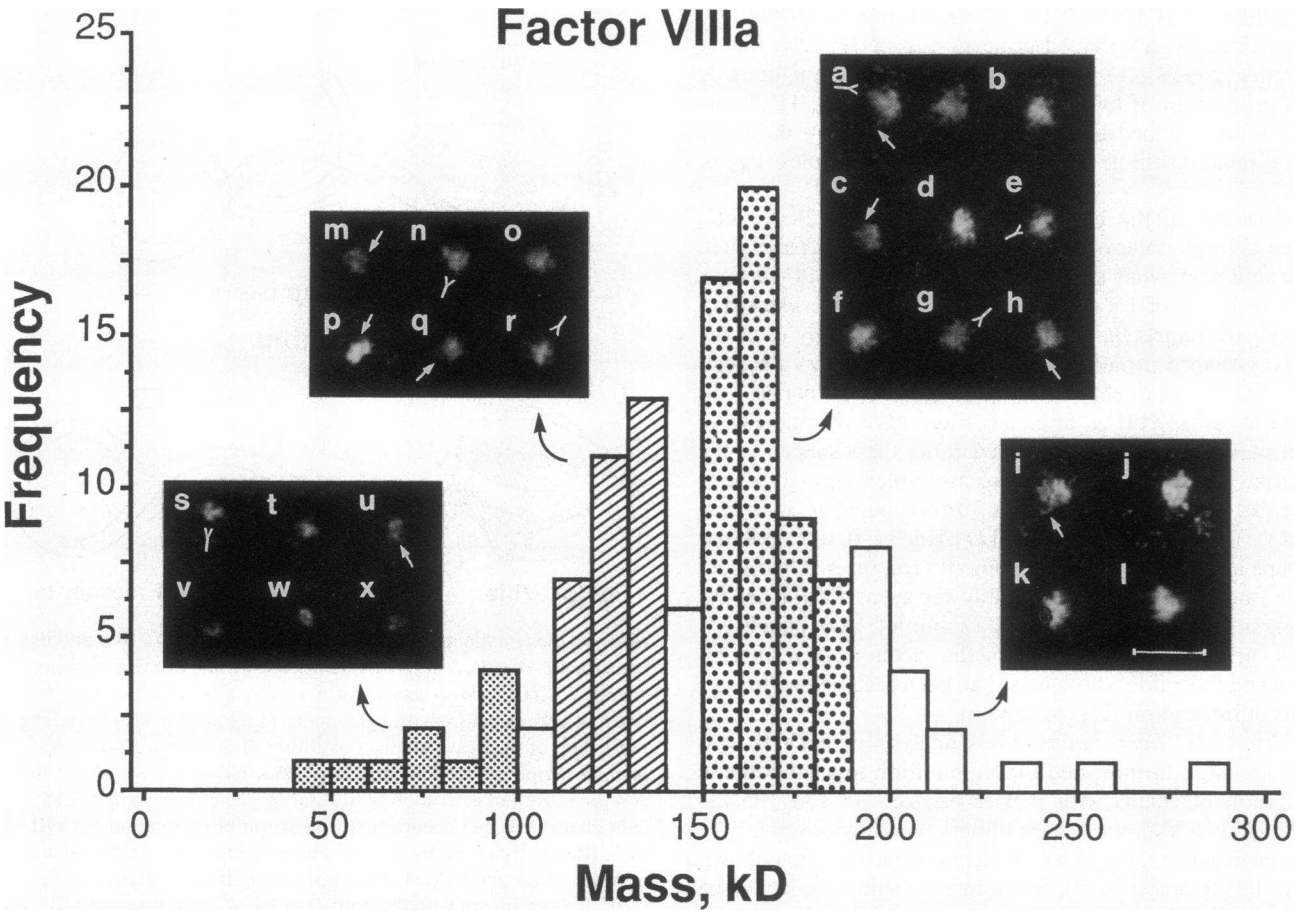

Figure 6. STEM images selected from fVIIIa preparations, and a frequency histogram of particles found in the preparation (r_i 11 nm). The large *dot-filled bars* indicate the range of the particles selected for panels *a–h; unfilled bars* between 200 and 240 kD, panels *i–l;* the *striped bars,* panels *m–r; small dot-filled bars,* panels *s–x.* Fingerlike (*arrows*) and v-shaped (*split lines*) structures are indicated. Bar (panel *l*), 20 nm.

Evaluation of particles with masses between 120 and 200 kD revealed that there were two discernible molecular forms within this size range. The first had mass values of 180–200 kD and corresponded in shape and size to a fVIII heterodimeric core structure with a truncated heavy chain (e.g., Fig. 3, panel *a*—molecule *3;* panels *i* and *j*). The second form had masses between 128 and 162 kD and corresponded in size to large free heavy chains (i.e., A_1–A_2–B/, A_1–A_2–B). These particles were irregularly globular and smaller (~ 8 nm) than the heavy chain/light chain core structures (Fig. 3, panel *a*—molecule *2;* panels *k–n*). One consistent aspect of these structures (seven of eight; 88%) was the presence of a bent fingerlike projection (e.g., Fig. 3, *arrow,* panels *a, k,* and *n*) corresponding in appearance to these seen at the periphery of fVIII core structures. Another feature was the presence of thin irregularly curled strands 1–2 nm wide, resembling the stalk of the satellite structure (e.g., Fig. 3, panel *a*—molecule *2,* panel *k*).

Mass analysis of a fVIII 82/76 preparation showed particles in a range of 35–400 kD (Fig. 5). The same mass distribution and particle shapes were observed whether or not 1 mM $CaCl_2$ was included in the specimen wash buffer (data not shown). Objects smaller than 120 kD probably reflect the presence of free heavy chains or light chains. Particles with masses above 220 kD were rare. Molecules in the 140–220-kD range had the same globular shape noted in fVIII 166/76 core structures, and commonly (13 of 30; 43%) possessed a fingerlike (Fig. 5, *arrows,* panels *a–c*) and/or v-shaped (9 of 30; 30%) projection (Fig. 5, *split line,* panel *b*). However, fVIII 82/76 molecules uniformly lacked the satellite structure seen in fVIII 166/76 molecules, and because of this, had a smaller mass (176±20 kD) that could be encompassed at an integration radius of 10 nm (Fig. 4) and that corresponded to the estimated size of heterodimers containing an $-A_3$–C_1–C_2 light chain and an A_1–A_2 heavy chain.

Factor VIIIa. Mass analysis of fVIIIa preparations revealed a polydisperse distribution of particles in a range of 40–290 kD (Fig. 6), and indicated that several populations of molecules were present. These corresponded to that expected for dissociated chains (40–100 kD), fVIIIa heterodimers (110–140 kD), fVIIIa heterotrimers (140–190 kD), and particles > 190 kD. The same mass distribution and particle shapes were observed whether or not 1 mM $CaCl_2$ was included in the specimen wash buffer (data not shown).

Molecules in the fVIIIa heterotrimer mass range appeared very similar in shape and size to the core structures observed in the fVIII 166/76 (Fig. 3) and fVIII 82/76 (Fig. 5) preparations, and none possessed a satellite appendage. Consequently, their mass was entirely encompassed at an r_i of 10 nm (162±13 kD; Fig. 4). Owing to irregular serrations in the contour of fVIIIa heterotrimers, plus the absence of a satellite structure to help

orient the location of peripheral core features, identification of a fingerlike (13 of 37; 35%; Fig. 6, *arrows,* panels *a, c,* and *h*), and particularly, a v-shaped projection (8 of 37; 22%; Fig. 6, *split lines,* panels *a, e,* and *g*) was sometimes ambiguous. A small proportion of fVIIIa heterotrimers (4 of 37; 11%) possessed both v-shaped and fingerlike appendages in the same general relationship as was found in fVIII molecules (Fig. 6, panel *a*).

Molecules in the heterodimer mass range (128±13 kD) tended to be globular or sometimes oblong (Fig. 6, panel *p*) in shape and somewhat smaller than heterotrimers (8–10 nm). Commonly (13 of 16; 80%) they possessed a fingerlike structure (Fig. 6, panels *m, p,* and *q*), or less commonly (3 of 16; 19%) a v-shaped projection (Fig. 6, panels *n* and *r*). Particles < 100 kD varied in shape from globular (Fig. 6, panels *t, w,* and *x*) to c-shaped (Fig. 6, panels *s* and *v*) or oblong (Fig. 6, panel *u*), and commonly displayed either the v-shaped or the fingerlike feature characteristic of assembled core structures and fVIII subunit chains (Fig. 6, *arrow,* panel *u; split line,* panel *s*). The few particles > 190 kD (panels *i–l*), were globular in shape and resembled heterotrimeric structures. Their identity is uncertain but they probably represent fVIIIa heterotrimers in association with a fVIIIa subunit (Fig. 6, panels *i, k,* and *l*), or a molecule situated in the vicinity of an uncomplexed small peptide whose mass had been included within the radius of integration (Fig. 6, panel *j*).

Factor VIII light chains. Mass analysis of a fVIII light chain preparation indicated that in addition to a monomeric population of chains with masses between 45 and 105 kD (mean, 76±16 kD), there were dimeric and higher-order light chain aggregates, some of which were outside the range shown in the histogram (Fig. 7). Monomeric chains tended to be c-shaped (Fig. 7, panels *a–c*) or irregularly globular (Fig. 7, panels *d–f*) structures 6–8 nm across. Commonly, a v-shaped projection (7 of 30; 23%) was evident (Fig. 7, panels *b, d,* and *e*) and appeared to originate from the middle region of the chain.

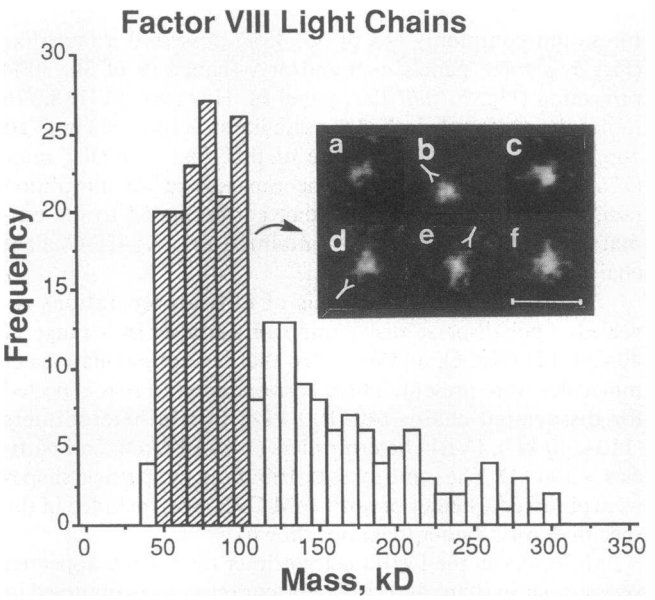

Figure 7. STEM images selected from a fVIII light chain preparation, plus a frequency histogram of the mass of particles found in the preparation (r_i 10 nm). The *striped bars* indicate the range of particles selected. The *split lines* indicate v-shaped structures. Bar (panel *f*), 20 nm.

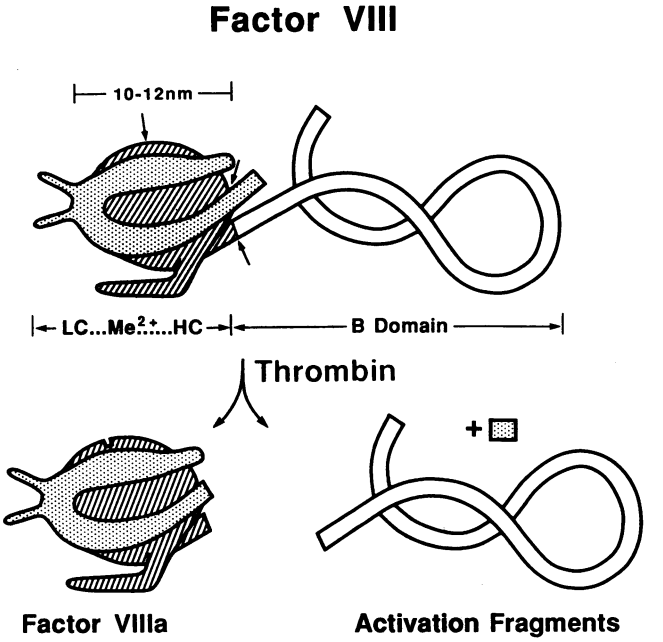

Figure 8. Schematic model of the structure of fVIII, fVIIIa, and its constituents based upon these studies. The A_1–A_2 domains of heavy chains (*HC*) (*striped structure*) form a compact divalent cation–dependent core structure with light chains (*LC*) (*dotted structure*). The remainder of the heavy chain constituting B domainal sequences forms a peripheral satellite structure that is cleaved (*arrow*) from the core as a result of activation by thrombin. Other heavy chain and light chain cleavages occurring during thrombin activation of fVIII to fVIIIa are indicated by arrows. The precise folding arrangements of heavy chain and light chains constituting the core structure of fVIII are not known with certainty, but based upon the observed subdomainal features of fVIII core structures and their identification as features of light chains (v-shaped projection) and heavy chains (fingerlike projection) their relative orientations can be suggested.

Such "precursor" fVIII light chains resembled c-shaped particles corresponding in shape and mass to dissociated fVIIIa light chains (e.g., Fig. 6, panel *s*, 74 kD).

Discussion

Porcine plasma fVIII heterodimers are composed of a heterogeneous population of heavy chains, ranging in molecular weight from 166,000 to 82,000 plus a light chain of mol wt 76,000 ($-A_3$–C_1–C_2) (5, 6) (Fig. 1). These forms of fVIII, including the porcine 82/76 species and those of human origin, require proteolytic activation to participate as a cofactor for factor IXa during the activation of factor X (7). The B domain does not appear to have a coagulant function since plasma-derived fVIII heterodimers lacking this domain have similar coagulant potential as B domain-containing heterodimers (7) and since deletion of most of the B domain from recombinant human fVIII by site-directed mutagenesis does not abolish coagulant potential (28, 29). Activation of porcine fVIII to fVIIIa by thrombin is accompanied by cleavages between the A_1 and A_2 domains, between the A_2 and B domains, and within the light chain near the amino terminus to produce a 69,000-mol wt derivative (A_3–C_1–C_2) (5, 6). The resulting heterotrimeric fVIIIa molecule consists of the A_1, A_2, and A_3–C_1–C_2 domains (15). These present studies coupling mor-

phological and mass analysis of high resolution STEM images, have provided the first detailed views of the ultrastructure of these molecules, and have enabled us to propose a model of the structure of fVIII and its activation product, fVIIIa (Fig. 8).

Mass analyses of fVIII molecules confirmed the molecular weight value determined by physical measurements or that predicted by summation of its constituent subunits (Table I). They indicate that components of fVIII 166/76 molecules extend well beyond the vicinity of its core structure (Fig. 4). These observations indicate that fVIII 166/76 molecules consist of a compact globular core of 10–12 nm that accounts for ~ 75% of its total mass, plus a peripheral satellite structure connected to it by a thin stalk, that accounts for the remainder. Factor VIII 82/76 molecules consist of a core structure that is indistinguishable from that of fVIII 166/76, but they lack a satellite structure, and thus their mass is fully accounted for by the core structure itself (Fig. 4). These findings clearly indicate that the A_1–A_2 heavy chain and the light chain components of the fVIII procofactor molecule are closely associated with one another to form the globular core structure, whereas the B domainal portion of the heavy chain is represented by the peripheral satellite appendage.

Factor VIIIa molecules consisted of several populations corresponding in mass to heterotrimers, heterodimers, and dissociated subunits. Molecules in the heterotrimer range were very similar in shape and size to the fVIII core structures, and none possessed a satellite appendage. Thus the globular structure comprising fVIIIa heterotrimers is derived directly from the heavy chain and light chain components of the fVIII core structure.

There were two subdomainal structures observed in fVIII core molecules: a fingerlike projection arising in the vicinity of the B domainal stalk and a v-shaped appendage situated opposite to the origin of the stalk. Visualization of these structures in any given molecule depends upon their proper extension in profile from the core and/or upon appropriate orientation of molecules on the grid surface, and could account for the relatively small proportion of molecules (26–30% in fVIII 166/76) displaying such features. V-shaped structures, in particular, are thinner and less dense than fingerlike structures, and may be more readily subject to beam damage, or more difficult to appreciate above the background noise from the carbon film itself, or both. Additionally, even when properly positioned, these features may become obscured or their identification made more ambiguous when the B domain is superimposed upon the core structure, such as sometimes occurs in fVIII 166/76 molecules (e.g., Fig. 3, panel *d*).

As assessed by STEM mass analysis, there were free large heavy chains in fVIII 166/76 preparations. These chains were smaller and more irregular than fVIII core structures, and possessed irregularly curled strands resembling the stalk of the B domainal satellite structure. A fingerlike projection was a prominent and consistent feature of these chains and closely resembled the fingerlike structure seen in fVIII core molecules, indicating that they represent the same region of the fVIII molecule.

Factor VIII light chains (–A_3–C_1–C_2), which encompass the carboxy-terminal region of the molecule, tend to have a c-shape which seems to be preserved in free light chains (A_3–C_1–C_2) found in fVIIIa preparations (e.g., Fig. 6, panel *s*). Owing to the small differences in size between fVIII and fVIIIa light chains, we cannot distinguish them from one another by this type of analysis. A v-shaped projection is a feature of both fVIII as well as fVIIIa light chains, and can also be identified at the periphery of assembled core structures in fVIII 166/76, positioned opposite to the stalk of the satellite appendage. These observations permit us to suggest the orientation of light chains in fVIII core molecules relative to its heavy chains (Fig. 8), based upon (*a*) the relative positions of v-shaped and fingerlike projections in core structures and (*b*) the assumption that uncomplexed light chains retain the same general shape as they do when they are complexed with heavy chains. The same two features were detected in some fVIIIa molecules in the same relative positions. This observation is consistent with the notion that the basic arrangements of light and heavy chains are preserved in the conversion of fVIII to fVIIIa; this issue will require further investigation.

As assessed by mass analysis, free heavy chains and free light chains were evidently present not only in images of fVIII 166/76 preparations but also in fVIII 82/76 preparations. We have also detected them in images of immunoaffinity purified fVIII preparations before mono S or mono Q chromatography (data not shown). They occur as well in fVIII preparations in which the specimen wash buffer contained 1 mM $CaCl_2$, thus eliminating the possibility that the absence of calcium ions, per se, from buffer solutions during specimen preparation might have contributed to their generation from heterodimeric forms during processing. It is possible that dissociation of heavy and light chains occurs after specimen dilution for application to the EM grids, and that their appearance represents a sort of dilutional "artifact." This would be consistent with the observation that multiple boundaries have not been observed during analytical velocity sedimentation of fVIII 166/76 preparations (30). It is interesting to note in this context that we have made several attempts to prepare fVIII heavy chains for EM analysis by releasing them from W3-3 affinity columns with EDTA-containing buffer solutions. These attempts at imaging monomeric chains have been uniformly unsuccessful, in that at most, we have observed aggregates of protein (data not shown). It may be that heavy chains have a tendency to self-associate in the absence of light chains.

Based upon ultracentrifugal analyses of fVIIIa (15), it seems likely that the fVIIIa preparations we studied exist in stock solution mainly as heterotrimers. Sedimentation equilibrium experiments at loading concentrations of 60–160 μg/ml showed a concentration dependent increase in apparent molecular weight from 148,000 to 161,000 (15). Sedimentation velocity analyses carried out at a concentration of 50 μg/ml revealed a single boundary sedimenting at 7.2S, thus excluding the possibility that there were large amounts of free light chains or heavy chain fragments in the preparation. STEM mass analysis of fVIIIa preparations indicated that heterotrimers were the predominant form, but heterodimers and dissociated subunits were also present in substantial amounts. Heterotrimeric fVIIIa structures resembled fVIII core structures, both in shape and submolecular detail. Heterodimers tended to be smaller than heterotrimers but many retained the heavy chain or light chain landmark features of heterotrimeric or fVIII core structures from which they had originated. Considering the characteristics of the fVIIIa stock solutions as summarized above, it seems that the molecular heterogeneity we observed in our STEM images of fVIIIa is the result, to some extent, of subunit dissociation occurring during specimen dilution and washing that accompany processing for subsequent STEM imaging.

The model we have proposed for fVIII and fVIIIa molecules should provide a useful tool for investigating and refining our understanding of the functional features of their domains, the nature of their complexation with other molecules, and for comparing their structure with that of other related proteins such as factor V (31, 32). Given the high degree of sequence and functional homology between fVIII and fV molecules, it is no surprise that their structures resemble one another. However, there are some noteworthy differences. The satellite structures (B domains) of fV molecules tend to extend further from the core structure than those of fVIII (up to 35 nm vs. up to 14 nm). More importantly, in contrast to fVIIIa, there is evidence for only a small degree of dissociation of factor Va molecules. Perhaps the tendency for fVIIIa molecules to dissociate can explain the instability of fVIIIa activity compared with that of fVa.

Acknowledgments

We are most grateful to Angela Mallett and Joy Reeve for their help in preparing the manuscript, to Susan Schuder and Karen Mickey for their graphic arts services, and to William Semrad for photographic services. We also thank Lynda Fleming and Nancy Kirschbaum for their critical review of this manuscript.

This investigation was supported by National Heart, Lung and Blood Institute Program Project grants HL-28444 and HL-17430, by National Institutes of Health grant RR-01777 to the Brookhaven STEM National Biomedical Resource Facility, by a National Institutes of Health SCOR Thrombosis grant HL-35058, and by an American Heart Association Established Investigator Award to Dr. Lollar.

References

1. Vehar, G. A., B. Keyt, D. Eaton, H. Rodriguez, D. P. O'Brien, F. Rotblat, H. Oppermann, R. Keck, W. I. Wood, R. N. Harkins, et al. 1984. Structure of human factor VIII. 1984. *Nature (Lond.).* 312:337–342.

2. Toole, J. J., J. L. Knopf, J. M. Wozney, L. A. Sultzman, J. L. Buecker, D. D. Pittman, R. J. Kaufman, E. Brown, C. Shoemaker, E. C. Orr, et al. 1984. Molecular cloning of a cDNA encoding human antihaemophilic factor. *Nature (Lond.).* 312:342–347.

3. Pittman, D. D., and R. J. Kaufman. 1988. Structure-function relationships of factor VIII elucidated through recombinant DNA technology. *Proc. Natl. Acad. Sci. USA.* 85:2429–2433.

4. Kaufman, R. J., L. C. Wasley, and A. J. Dorner. 1988. Synthesis, processing, and secretion of recombinant human factor VIII expressed in mammalian cells. *J. Biol. Chem.* 263:6352–6362.

5. Fass, D. N., G. J. Knutson, and J. A. Katzmann. 1982. Monoclonal antibodies to porcine factor VIII coagulant and their use in the isolation of active coagulant protein. *Blood.* 59:594–600.

6. Lollar, P., G. J. Knutson, and D. N. Fass. 1984. Stabilization of thrombin-activated porcine factor VIII:C by factor IXa and phospholipid. *Blood.* 63:1303–1308.

7. Fay, P. J., M. T. Anderson, S. I. Chavin, and V. J. Marder. 1986. The size of human factor VIII heterodimers and the effects produced by thrombin. *Biochim. Biophys. Acta.* 871:268–278.

8. Fulcher, C. A., and T. S. Zimmerman. 1982. Characterization of the human factor VIII procoagulant protein with a heterologous precipitating antibody. *Proc. Natl. Acad. Sci. USA.* 79:1648–1652.

9. Rotblat, F., D. P. O'Brien, F. J. O'Brien, A. H. Goodall, and E. G. D. Tuddenham. 1985. Purification of human factor VIII:C and its characterization by western blotting using monoclonal antibodies. *Biochemistry.* 24:4294–4300.

10. Hamer, R. J., J. A. Koedam, N. H. Beeser-Visser, and J. J. Sixma. 1986. Human factor VIII: purification from commercial factor VIII concentrate, characterization, identification and radiolabeling. *Biochim. Biophys. Acta.* 873:356–366.

11. Hoyer, L. W., and N. C. Trabold. 1981. The effect of thrombin on human factor VIII. *J. Lab. Clin. Med.* 97:50–64.

12. Weinstein, M. J., and L. E. Chute. 1984. Two distinct forms of factor VIII coagulant protein in human plasma. *J. Clin. Invest.* 73:307–316.

13. Aronson, D. L., J. W. Preiss, and M. W. Mosesson. 1962. Molecular weights of factor VIII (AHF) and factor IX (PTC) by electron irradiation. *Thromb. Diath. Haemorrh.* 8:270–275.

14. Harmon, J. T., G. A. Jamieson, and G. A. Rock. 1982. The functional molecular weights of factor VIII activities in whole plasma as determined by electron irradiation. *J. Biol. Chem.* 257:14245–14249.

15. Lollar, P., and C. G. Parker. 1989. Subunit structure of thrombin-activated porcine factor VIII. *Biochemistry.* 28:666–674.

16. Fay, P. J. 1987. Subunit structure of thrombin-activated human factor VIIIa. *Biochim. Biophys. Acta.* 952:181–190.

17. Hultin, M. B., and Y. Nemerson. 1978. Activation of factor X by factors IXa and VIII: a specific assay for factor IXa in the presence of thrombin-activated factor VIII. *Blood.* 52:928–940.

18. Rick, M. E., and L. W. Hoyer. 1977. Thrombin activation of factor VIII: effect of inhibitors. *Br. J. Haematol.* 36:585–597.

19. Vehar, G. A., and E. W. Davie. 1977. Formation of a serine enzyme in the presence of bovine factor VIII (antihemophilic factor) and thrombin. *Science (Wash.DC).* 197:374–376.

20. Cooper, H. A., F. F. Reisner, M. Hall, and R. H. Wagner. 1975. Effects of thrombin treatment on preparations of factor VIII and the Ca^{2+}-dissociated small active fragment. *J. Clin. Invest.* 56:751–760.

21. Hultin, M. B., and J. Jesty. 1981. The activation and inactivation of human factor VIII by thrombin: effect of inhibitors of thrombin. *Blood.* 57:476–482.

22. Lollar, P., C. G. Parker, and R. P. Tracy. 1988. Molecular characterization of commercial porcine factor VIII concentrate. *Blood.* 71:137–143.

23. Mosesson, M. W., J. Hainfeld, R. H. Haschemeyer, and J. Wall. 1981. Identification and mass analysis of human fibrinogen molecules and their domains by scanning transmission electron microscopy. *J. Mol. Biol.* 153:695–718.

24. Wall, J. S., and J. F. Hainfeld. 1986. Mass mapping with the scanning transmission electron microscope. *Annu. Rev. Biophys. Biophys. Chem.* 15:355–376.

25. Hainfeld, J. F., J. S. Wall, and E. J. Desmond. 1982. A small computer system for micrograph analysis. *Ultramicroscopy.* 8:263–270.

26. Wall, J. 1979. Biological scanning transmission electron microscopy. *In* Introduction to Analytical Electron Microscopy. J. J. Hren, J. J. Goldstein, and D. C. Joy, editors. Plenum Publishing Corp., New York. 333–342.

27. Wall, J. 1979. Limits on visibility of single heavy atoms in the scanning transmission electron microscope—an experimental study. *Chem. Scr.* 14:271–278.

28. Toole, J. J., D. D. Pittman, E. C. Orr, P. Murtha, L. C. Wasley, and R. J. Kaufman. 1986. A large region (approximately equal to 95 kDa) of human factor VIII is dispensible for in vitro procoagulant activity. *Proc. Natl. Acad. Sci. USA.* 83:5939–5942.

29. Eaton, D. L., W. I. Wood, D. Eaton, P. E. Hass, P. Hollingshead, K. Wion, J. Mather, R. M. Lawn, G. A. Vehar, and C. Gorman. 1986. Construction and characterization of an active factor VIII variant lacking the central one-third of the molecule. *Biochemistry.* 25:8343–8347.

30. Lollar, P., and C. G. Parker. 1987. Stoichiometry of the porcine factor VIII-von Willebrand factor association. *J. Biol. Chem.* 262:17572–17576.

31. Mosesson, M. W., M. E. Nesheim, J. DiOrio, J. F. Hainfeld, J. S. Wall, and K. G. Mann. 1985. Studies on the structure of bovine factor V by scanning transmission electron microscopy. *Blood.* 65:1158–1162.

32. Mosesson, M. W., W. R. Church, J. P. DiOrio, S. Krishnaswamy, K. G. Mann, J. F. Hainfeld, and J. S. Wall. 1990. Structural model of factors V and Va based on scanning transmission electron microscope images and mass analysis. *J. Biol. Chem.* In press.